AJNR

Role of MR Imaging in Prenatal Diagnosis of Pregnancies at Risk for Joubert Syndrome and Related Cerebellar Disorders

S.N. Saleem and M.S. Zaki

AJNR Am J Neuroradiol published online 26 November 2009
http://www.ajnr.org/content/early/2009/11/26/ajnr.A1867.citation

Published November 26, 2009 as 10.3174/ajnr.A1867

ORIGINAL RESEARCH

Role of MR Imaging in Prenatal Diagnosis of Pregnancies at Risk for Joubert Syndrome and Related Cerebellar Disorders

S.N. Saleem
M.S. Zaki

BACKGROUND AND PURPOSE: JSRD are rare autosomal recessive brain malformations. We hypothesized that MR imaging can assess fetuses at risk for JSRD and might influence their diagnoses.

MATERIALS AND METHODS: We prospectively performed cranial MR imaging for 12 fetuses (mean GA, 23 weeks; SD, 3.7) at 25% recurrence risk for JSRD. We correlated prenatal MR imaging findings with postnatal MR imaging and clinical outcome. Retrospectively, we compared posterior fossa measurements of the cases with those of 24 age-matched fetuses with proved normal brain MR imaging. Institutional review board approval and consents were obtained. Statistical methods included a *t* test and ANCOVA tests.

RESULTS: Fetal MR imaging correctly diagnosed 3 cases at 22, 28, and 29 weeks of gestation as JSRD, and 9 cases as normal. In JSRD-affected fetuses, prenatal MR imaging detected narrow pontomesencephalic junction (isthmus) with deepening of the interpeduncular fossa and thick horizontally placed superior cerebellar peduncles (MTS), deformed anteriorly convex floor of the fourth ventricle, and midline cerebellar cleft in place of the hypoplastic vermis. Measurements on axial fetal MR imaging at pontomesencephalic junction, ratio of AP diameters of interpeduncular fossa to midbrain/isthmus, and ratio of the AP to transverse diameters of the fourth ventricle were significantly higher in JSRD-affected fetuses than in nonaffected cases and the control group.

CONCLUSIONS: MR imaging can diagnose JSRD in at-risk pregnancies by detecting posterior fossa signs. Measurements at the pontomesencephalic junction may enhance fetal MR imaging accuracy in diagnosing JSRD.

ABBREVIATIONS: ANCOVA = analysis of covariance; AP = anteroposterior; CM = cisterna magna; COACH syndrome = cerebellar vermis hypoplasia/aplasia, oligophrenia, ataxia, coloboma, and hepatic fibrosis syndrome; CORS = cerebello-oculo-renal syndrome; DWM = Dandy-Walker malformation; ERG = electroretinograms; GA = gestational age; IP = interpeduncular fossa; OFD-VI = orofacial-digital type VI syndrome; JS = Joubert syndrome; JSRD = Joubert syndrome and related cerebellar disorders; US = ultrasonography; MRI = MR imaging; MTS = molar tooth sign; VEP= visual-evoked potentials

Joubert syndrome and related cerebellar disorders are a .group of rare autosomal recessive conditions characterized primarily by hypotonia, ataxia, developmental delay, abnormal respiratory pattern, and ocular movement abnormalities.[1,2] Variable combinations of central nervous system, respiratory, renal, and eye anomalies were reported with the 4 major subtypes of JSRD: classical JS, COACH, CORS, and OFD-VI.[3,4]

MR imaging plays the cornerstone in establishing the diagnosis of JSRD. MTS is the cardinal diagnostic sign visualized on axial imaging at the pontomesencephalic junction in almost all cases of JSRD.[5-9] MTS describes narrow isthmus, deep interpeduncular fossa, and thick horizontally placed superior cerebellar peduncles.[5-7] Other MR imaging signs include a midline cerebellar cleft in place of the hypoplastic vermis on coronal images, as well as the characteristic anteriorly convex floor of the fourth ventricle on axial images.[6,8,9]

The prognosis of JSRD could be poor, as it is associated with severe mental and motor retardation in many cases.[10,11] Parents of a child with JSRD have a 25% chance of conceiving an affected fetus with each pregnancy.[4,12,13] For a woman pregnant with a fetus at risk for a devastating anomaly such as JSRD, prenatal diagnosis may facilitate informed reproductive choices, reduce anxiety through reassurance, or enable preparations for the birth of an affected child.[14]

The genetic basis of JSRD includes a diverse set of 3 causative genes and 2 other unique loci where the genes have not yet been identified. Mutations of one of the causative genes of Meckel-Gruber syndrome, *MKS3*, have also been found recently in patients with classical JS and CORS.[13] This genetic heterogeneity makes a molecular prenatal diagnosis in JSRD a challenge.[15] Amniocentesis and chorionic villus sampling are not helpful in JSRD because DNA and protein markers for most types are not widely available on a clinical basis.[13]

Prenatal US diagnosis of JSRD has proved difficult because of the known limitations in US imaging of the fetal posterior fossa, the rarity of the condition, and the relatively nonspecific findings reported in most affected fetuses.[16-20]

Fetal MR imaging is now acknowledged as the method of

Received June 23, 2009; accepted after revision August 5.

From the Radiology Department (S.N.S.), Kasr Al-Ainy Hospital, Cairo University, Cairo, Egypt; and Clinical Genetics Department (M.S.Z.), Human Genetics and Genome Research Division, National Research Centre, Cairo, Egypt.

Please address correspondence to Sahar N. Saleem, Kasr Al-Ainy Hospital, Radiology Department, Cairo University, 4 St 49 Mokkattam, Cairo 11571, Egypt; e-mail: saharsaleem1@gmail.com

Indicates article with supplemental on-line table

DOI 10.3174/ajnr.A1867

choice to delineate posterior fossa malformations in a fetus.[21-23] However, MR imaging findings in fetuses at risk for JSRD were only reported in the literature in 2 case reports.[24,25] The positive and negative predictive values of MR imaging findings for diagnosing JSRD in utero are not yet known.[17,19,24]

We hypothesized in this study that MR imaging can assess fetuses at risk for JSRD and might influence their diagnoses.

Materials and Methods

Patients

The patients were enrolled in a sequential fashion in the Genetics Clinic at National Research Centre, Cairo, Egypt, between June 2004 and May 2008, from families meeting inclusion criteria for JSRD in this institutional review board-approved study. The inclusion criteria included a family member or more with the typical MTS brain imaging finding in addition to clinical evidence of the syndrome (hypotonia and developmental delay, accompanied by either abnormal breathing or abnormal eye movement). No exclusion criteria were specified. Twelve fetuses with a mean GA of 23 weeks (SD 3.7; range, 18–30; median, 22) from 12 Egyptian families were studied. The mean age of the mothers was 30.2 years (SD 5.7). Eight families were first-cousin marriages, 2 had more distant documented consanguinity, and negative consanguinity was reported in 2 families. Seven of the families had more than a single affected member. In no instance was there a symptomatic parent. JSRD phenotypes were ascertained in all of the affected family members. The classical form of the JS was documented in 11 families with its characteristic clinical features of hypotonia, psychomotor delay, oculomotor apraxia, neonatal breathing dysregulation, pigmentary retinal changes, and polydactyly; COACH was diagnosed in 1 family with cerebellar vermis hypoplasia, oligophrenia, ataxia, coloboma, and hepatic fibrosis. The on-line Table shows the clinical and imaging data of the classical JS-affected family members. Brain MR imaging studies of all of the classic JS-affected family members showed the characteristic MTS. Brain abnormalities other than MTS were brain stem hypoplasia in JSRD-affected family members of case 4, as well as unilateral polymicrogyria and thin corpus callosum in JSRD-affected family members of case 8.

All of the cases were referred with detailed fetal 2D and 3D neurosonographic studies that were performed 0 to 5 days (average, 3; SD 1.5) before MR imaging by physicians experienced in fetal US imaging by using 2.5–5.0 MHz transducers of Accuvix XQ (Medison, Seoul, Korea) or Voluson E8 (GE Healthcare, Milwaukee, Wisconsin) sonography scanners. Vaginal US scans with 4–8- or 6–12-MHz transducers were attempted when the fetus was in cephalic position. US studies were done with knowledge of the patient's history. The on-line Table includes the referred prenatal US findings of the 12 fetuses at high risk for JSRD: 7 fetuses were diagnosed as normal; 3 fetuses had equivocal US findings where no brain abnormalities were detected or could be ruled out due to inability to obtain a midsagittal image or reverberating artifacts of the posterior fossa; 1 fetus had a suspicious prominent CM (9 mm); and 1 fetus had equivocal neurosonographic findings of the posterior fossa but JSRD was suspected upon detection of polydactyly.

Fetal MR Imaging Technique

Written consents were obtained from the mothers of the studied fetuses and control group. Fetal MR imaging was performed with a 1.5T superconducting magnet (Intera; Philips Medical Systems, Best, the Netherlands) and a phased-array surface coil. No patients were excluded because of contraindication to MR imaging or claustrophobia. Brain images were obtained in multiple planes by using T2-weighted balanced fast-field echo (Philips proprietary version of steady-state free precession) with TR/TE of 3.5–4 ms/1.7–2 ms, FA of 60–90, 2 signals acquired, 256 × 256 matrix, and 4-mm section thickness without intersection gap. No contrast agents or sedatives were used. All fetal MR imaging studies were interpreted by the radiologist in this study with more than 18 years of experience in neuroimaging and more than 8 years of experience in fetal MR imaging. The MR images of the 12 fetuses at risk for JSRD were assessed for posterior fossa abnormalities commonly reported in JSRD: MTS, dysplastic vermis, midline cerebellar cleft in place of the hypoplastic vermis on coronal images, and the characteristic anteriorly convex floor of the fourth ventricle on axial images. Fetal MR images were also assessed for any associated brain abnormalities. For definitive diagnosis, we correlated fetal MR imaging findings with detailed postnatal clinical examination.

Outcome Measures

The expectant parents and their referring physicians were informed of the results of the fetal MR imaging with the caveat that the study is investigative and of unproven accuracy for diagnosing JSRD. All live births underwent postnatal assessment within the first month of life that was repeated at 12–24 months of age supervised by the pediatrician-geneticist in this study with 20 years of experience. Postnatal examination included detailed physical and neurologic assessment with particular attention to findings commonly seen in JSRD, such as characteristic tachypnea-apnea spells, abnormal eye movements (skew deviations and nystagmus), and abnormal muscle tone (hypotonia). Postnatal assessment included a standard developmental profile to detect for any psychomotor delay; blood chemistry tests for elevations in blood urea nitrogen, creatinine, and liver transaminases to evaluate for evidence of impaired organ function; abdominal US to detect for any renal or hepatic abnormalities; and a baseline eye examination to test for retinal dysplasia and coloboma. When visual problems were suspected, VEP study and ERG were done. Infants who showed abnormal physical signs or delayed development had a detailed brain MR imaging.

According to the final diagnosis, the 12 studied cases were grouped as either JSRD-affected or JSRD-nonaffected.

Retrospectively, we obtained multiple posterior fossa measurements in the prenatal MR imaging of both groups (JSRD-affected and JSRD-nonaffected). The initial fetal MR imaging and the subsequent measurements of the posterior fossa were assessed by the neuroradiologist in this study. On a midsagittal imaging, we measured the maximum AP diameter of the CM as well as the maximum superior-inferior diameter of the vermis. On axial images showing the cerebellum, we measured the maximum transverse cerebellar diameters. On axial images at the level of lower midbrain-pontomesencephalic junction, where abnormalities are commonly seen in JSRD, we measured the AP diameter of IP fossa, AP diameter of the midbrain/isthmus, as well as the AP and transverse diameters of the fourth ventricle. We calculated the ratio between measurements at the pontomesencephalic junction (AP of IP fossa to AP of isthmus as well as AP to transverse diameters of the fourth ventricle) to quantify morphologic changes of the structures at this level. We correlated the measurements with those of normal fetuses at the same GA available in fetal biometry.[26-28]

We compared MR imaging measurements obtained in fetuses at risk for JSRD with those of 24 age-matched fetuses (average, 22.2 weeks; SD 3.3; range, 18–30; median, 21.5) with normal in utero brain MR imaging studies that were confirmed by normal detailed postnatal clinical and neurologic examination at an average age of 15.5

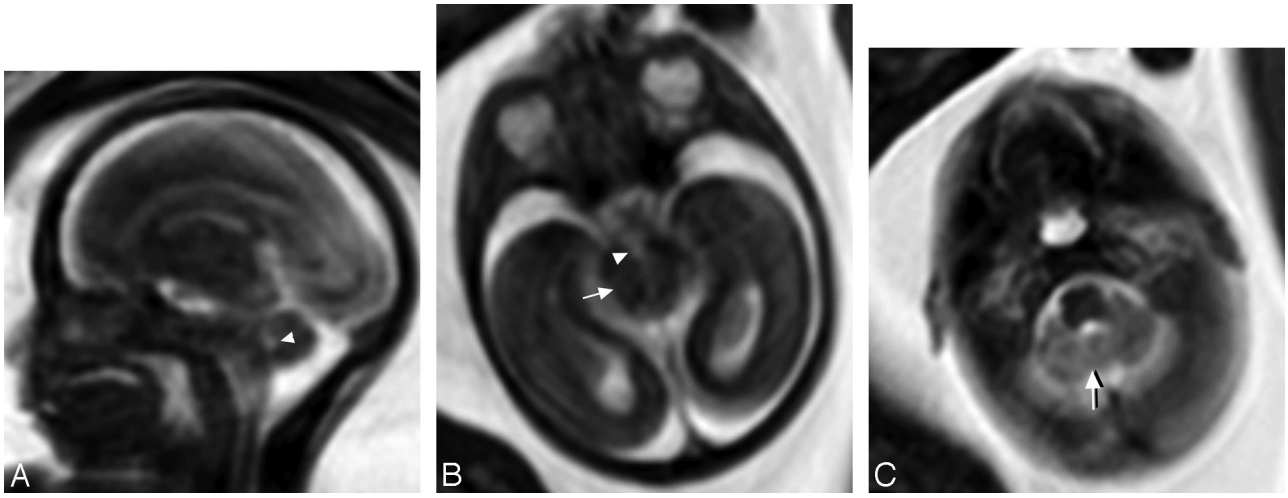

Fig 1. Female fetus at 20 weeks of gestation at risk of JSRD with normal brain in fetal MR imaging and a normal postnatal outcome. *A,* Prenatal midline sagittal MR image shows a normal fourth ventricle (*arrowhead*). The midline cerebellum appears intact and the CM is not dilated. *B,* Prenatal axial MR image through the level of the lower midbrain shows that the AP diameter of the IP fossa (*arrowhead*) is smaller than that of the midbrain (isthmus) (*arrow*). *C,* Prenatal axial MR image at the level of the pons shows a normal-sized fourth ventricle. Midline vermian tissues appear between the 2 cerebellar hemispheres (*arrow*). It is difficult to identify the normal superior cerebellar peduncles because of their small size and their downward oblique orientation

months (SD 5.3) and normal postnatal MR imaging done at an average age of 4.1 months (SD 2.3). Cases for the control group were selected from a large pool of participants in our study of MR imaging for at-risk pregnancies for brain anomalies.

Statistical Methods

We compared the MR imaging measurements obtained in the 3 groups by using independent 2-tailed *t* test. To control variation of GA in the studied cases, ANCOVA was used where the GA was the covariate, all of the MR imaging findings were the dependent test, and the affected group was the independent variable. A P value of <0.05 level was considered significant. Post hoc statistical power analysis was calculated. The statistical analysis was done by using SPSS, version 12 (SPSS, Chicago, Illinois).

Results

Prospectively, MR imaging diagnosed 9 fetuses as normal (Fig 1). The 9 cases showed normal physical and neurologic examinations during the first month of life as well as on follow-up clinical examinations until an average age of 16 months (SD 6).

In the other 3 fetuses, MR imaging showed suspected diagnosis of JSRD at 22 weeks (Fig 2), 30 weeks (Fig 3), and 28 weeks of gestation upon detection of MTS, a midline cerebellar cleft in place of the hypoplastic vermis on coronal images, and deformed anteriorly convex floor of the fourth ventricle on axial images. The MTS was mild in the 3 fetuses with a less notable affection of the superior cerebellar peduncles in the fetus diagnosed at 22 weeks (Fig 2*A*). AP diameter of the CM measured 11, 8, and 9 mm in fetuses diagnosed as JSRD-affected at 22 (case 2), 30 (case 6), and 28 weeks (case 9) of gestation, respectively. Superior-inferior diameters of cerebellar vermis were not reliably measured in JSRD-affected cases due to pseudovermis appearance of the cerebellar hemispheres at the midsagittal images (Fig 2*A*). There were no abnormal MR imaging findings related to the developing cerebral cortex, sulci, or supratentorial ventricles in any of the studied fetuses.

Postnatal examination of the 3 cases diagnosed as JSRD-affected with MR imaging showed 1 female and 2 males (cases 2, 6, and 9) with physical and neurologic examinations impressive of JSRD (on-line Table). Postnatal MR imaging of the 3 cases showed MTS without any associated abnormalities related to the cerebral cortex, sulci, corpus callosum, olfactory bulbs, optic tracts, or supratentorial ventricles.

Retrospective analysis of fetal MR imaging posterior fossa measurements in cases that were proved to be normal were statistically close to control group by using 2-tailed *t* test; the measurements matched also those of normal fetuses at corresponding GAs in fetal biometry.[26-28] By comparing the mean and ratios of posterior fossa measurements in the different groups, those of the JSRD-affected group were higher than those in JSRD-nonaffected fetuses and the control group. The mean AP diameter of the cisterna magna measured 9.3 mm (SD 1.5) compared with 7 mm (SD 2.2) in nonaffected cases and 6 mm (SD 1.1) in the control group. At the pontomesencephalic junction (Fig 3*C*), the mean ratio of AP diameter of the IP fossa to that of the midbrain/isthmus was significantly higher in JSRD-affected cases (0.9; SD 0.1) than in nonaffected cases (0.41; SD 0.04) and the control group (0.34; SD 0.08). The mean ratio of the AP to transverse diameters of the fourth ventricle was higher in JSRD-affected cases (1.65; SD 0.35) than in nonaffected cases (0.9; SD 0.2) and in the control group (0.9; SD 0.3).

Comparison between the JSRD-affected and control groups as well between JSRD-affected and nonaffected groups in the following MR imaging findings by using independent 2-tailed Student *t* test revealed: ratio of AP-to-transverse diameters of fourth ventricle ($P < .0001$ and .0001), AP diameter of CM ($P < .0001$ and .05), transverse cerebellar diameter ($P < .004$ and .003), superior-inferior diameter of vermis ($P < .029$ and .009), and IP-to-isthmus ratio ($P < .0001$ and .0001). Power analysis ranged from 65% to 75% for the JSRD-affected compared with nonaffected groups and from 70% to 80% for the JSRD-affected group compared with the normal controls. The effect size estimation ranged from 0.57 to 1.6 for the JSRD-affected group compared with the nonaffected groups

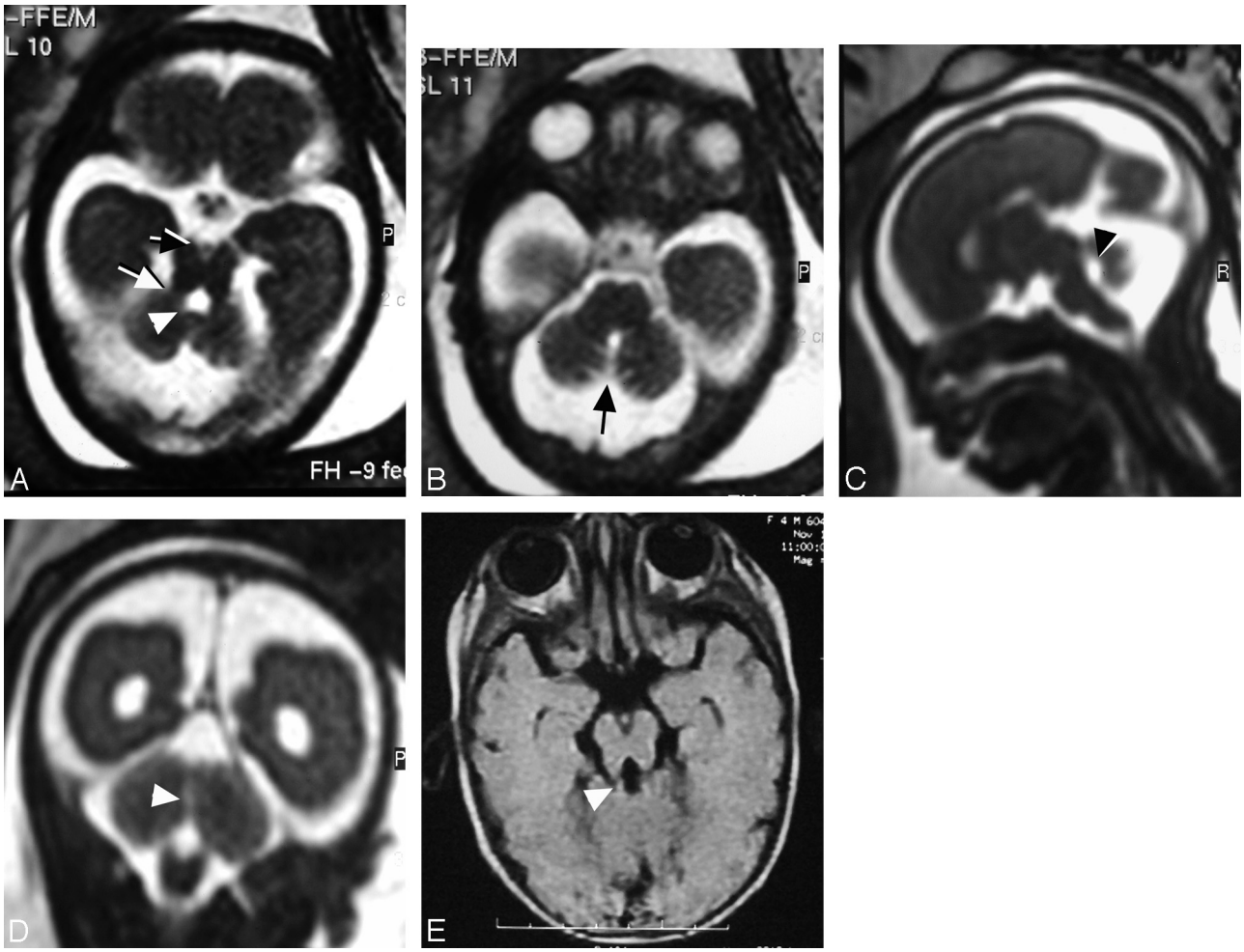

Fig 2. Female fetus at 22 weeks of gestation shows abnormal brain in MR imaging suggestive of JSRD. *A,* Prenatal axial MR image at the level of the pontomesencephalic junction shows the interpeduncular cistern (*black arrow*) deeper and wider than normal. The midbrain isthmus is abnormally narrowed in its AP diameter. The thick horizontal superior cerebellar peduncles (*white arrow*) represent the roots of the tooth for the MTS diagnostic of JSRD. There is dilation of the fourth ventricle (*arrowhead*) with a deformed anteriorly convex floor. *B,* Prenatal axial MR image at the level of the pons shows a midline sagittal CSF-containing cleft (*arrow*) separating the 2 cerebellar hemispheres denoting absent vermian tissues. *C,* Prenatal midsagittal MR image shows dilated CM, dilated fourth ventricle with rounding of its roof (*arrowhead*), and migration of the cerebellar hemispheres to the midline due to a hypoplastic/dysgenetic vermis. *D,* Prenatal coronal MR image shows the cerebellar hemispheres separated in the midline by sagittal cleft-containing CSF (*arrowhead*) caused by dysgenesis/agenesis of the vermis. *E,* Postnatal axial T1-weighted MR image at the age of 4 months documents JSRD diagnosis by showing a mild MTS (*arrowhead*).

and from 0.8 to 1.9 for JSRD-affected compared with control groups in the above-mentioned parameters.

An ANCOVA test suggested a strong relationship between the studied MR imaging findings and the JSRD-affected group controlling for GA at a P value of $<.05$ for the following MR imaging findings: AP diameter of the CM ($P < .008$), superoinferior diameter of vermis ($P < .0001$), IP fossa-to-isthmus ratio ($P < .0001$), ratio of AP-to-transverse diameters of the fourth ventricle ($P < .0001$), and maximum transverse cerebellar diameter ($P < .0001$). The ANCOVA test eliminated the potential effect of GA variation on the JSRD-affected group results.

Discussion

We report in this study 12 families with a history of siblings who were diagnosed with JSRD. Parents of a child with JSRD have a 25% chance of conceiving an affected fetus with each pregnancy.[3] Because inbreeding has been demonstrated to approximately double the rate of a recessive disease in a given population, JSRD are more commonly manifested in Egypt known with its high rate (30%–40%) of marriages in consanguineous couples.[12,13] Ten out of 12 families (83.3%) in our study had positive consanguinity, and 7 families (58.3%) had more than 1 affected sibling mostly with severe mental and motor retardation.

Difficulties in prenatal imaging of JSRD are attributed to the rarity of the condition (1/100,000 live births).[16-20] To the best of our knowledge, prenatal imaging of JSRD was described in the literature in only 14 fetuses, most of which were examined by US.[16,18,19,24,25,29-35] All fetuses at risk of JSRD in this study were referred with either normal or equivocal neurosonographic findings. Limitations of US imaging of fetal posterior fossa are widely reported.[36-38] Other studies documented significant discrepancies in sonographic prenatal diagnosis and postnatal diagnosis of posterior fossa malformations, especially vermian abnormalities.[38-40] Moreover, prenatal US findings in JSRD are relatively nonspecific and include dilated CM, vermian hypoplasia, occipital encephalocele, and ventriculomegaly.[16-20,24] US diagnosis of JSRD in utero usually relies on a positive family history and the finding of abnormal posterior fossa anatomy or the presence of asso-

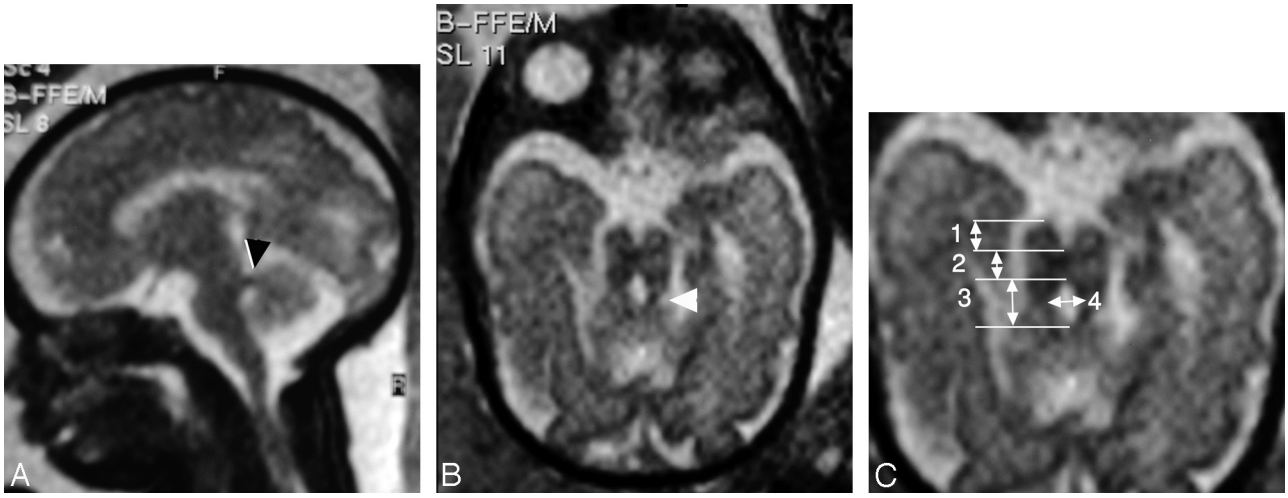

Fig 3. Male fetus at 30 weeks of gestation with abnormal brain MR imaging findings suggestive of JSRD. *A,* Prenatal sagittal MR image shows thick superior cerebellar peduncles at right angles to the posterior surface of the brain stem (*arrowhead*) suggesting JSRD. Note that the CM is not dilated. *B,* Prenatal axial MR image at the pontomesencephalic junction shows MTS (*arrowhead*). *C,* Measurements obtained in axial prenatal MR image at the lower midbrain/pontomesencephalic junction: the AP diameter of the interpeduncular fossa (no. 1), AP diameter of midbrain/isthmus (no. 2), as well as the AP (no. 3) and transverse (no. 4) diameters of the fourth ventricle. Note that the AP diameter of the interpeduncular fossa is almost equal to that of the narrow isthmus and the AP diameter of the superior aspect of the fourth ventricle is longer than its transverse diameter

ciated suggestive features such as kidney anomalies or polydactyly.[19,25] In this study, US suspected JSRD in a fetus upon detecting polydactyly rather than revealing brain abnormalities.

Fetal MR imaging does not suffer from the US imaging restraints and is now acknowledged as the method of choice in imaging the posterior fossa in utero.[23] In a recent study, Tilea and colleagues[41] found that both fetal MR imaging and fetopathology had similar performance with respect to the detection of vermian agenesis and brain stem abnormalities. The researchers concluded that a systematic analysis of the posterior fossa in fetal MR imaging makes it possible to diagnose accurately most noncystic posterior fossa malformations.[41]

Although fetal MR imaging is useful in diagnosing posterior fossa anomalies, its sensitivity in JS has not been systematically evaluated. To the best of our knowledge, a total of 3 fetuses at risk of JSRD were examined by MR imaging in 2 reports; 2 out of the 3 fetuses proved to be JSRD-affected, while the third case was normal.[24,25] In a report by Doherty and colleagues, fetal MR imaging suggested affection in a fetus at 21 weeks of gestation by showing vermian hypoplasia without being able to demonstrate a MTS.[24] Aslan and colleagues, too, diagnosed JSRD in utero by demonstrating vermis hypoplasia.[19] Vermis hypoplasia appears as a fluid communication between the fourth ventricle and the CM that persists after 18 weeks of gestation.[9] In the JSRD-affected fetuses in this study, a midline cerebellar cleft in place of the hypoplastic vermis on coronal images pointed to vermian hypoplasia (Fig 2*D*). Precise measurement of the midline cerebellum was not possible in the JSRD-affected fetuses due to herniation of cerebellar hemispheres at the midsagittal MR images, which gave a pseudovermis appearance and erroneous impression of intact midline cerebellum (Figs 2*C* and 3*A*). In the 3 JSRD-affected fetuses in this study, the CM was either mildly dilated or at the high limit of normal measurements (9.5 mm); this is in concordance with Doherty and colleagues' report[24] (Figs 2*C* and 3*A*). However, neither CM dilation nor vermian hypoplasia is pathognomonic of JSRD being shared with other posterior fossa malformations such as DWM, isolated vermian hypoplasia, pontocerebellar hypoplasia, and craniocerebellocardiac syndrome.[16-20]

MTS is considered the cardinal diagnostic imaging sign for JSRD.[5-7,9,13] In 1 study, the MTS was reported to be pathognomonic of this anomaly.[5] The underlying pathology of MTS is lack of normal decussation of superior cerebellar peduncular fibers that leads to enlarged peduncles that follow a more horizontal course between the midbrain and the cerebellum.[2] The absence of crossing fibers is responsible for the decreased anteroposterior diameter of the midbrain and causes the interpeduncular cistern to be deeper than that in the normal brain. The clinical manifestations in JSRD may be caused by the inability of the posterior fossa fiber tracts to cross the midline.[5] The identification of MTS by fetal MR imaging has been documented in literature in a single report at 27 weeks of gestation.[25] Fetal MR imaging identified MTS in all of the 3 JSRD-affected fetuses in our study as early as 22 weeks of gestation (Figs 2*A* and 3*B*). The thick horizontally oriented superior cerebellar peduncles, however, were more prominent in the 2 cases diagnosed later in gestation at 28 and 30 weeks (Fig 3*B*). Fetal MR imaging identified the fourth ventricular deformity in the JSRD-affected fetuses in this study. On sagittal MR images (Fig 2*C*), the fourth ventricle of the JSRD-affected fetuses was abnormally rounded and lacked the characteristic posterior point (fastigial point). Axial MR images (Fig 2*A*) showed the deformed anteriorly convex floor of the fourth ventricle, the appearance of which resulted from lack of decussation of the superior cerebellar peduncles in the tegmentum.[25]

For a couple who has already had a child with JSRD, presence of posterior fossa abnormality is significant; however, the absence of evident signs does not preclude a diagnosis because of the unknown sensitivity and because of possible intrafamilial variability.[24,25] Aiming at identification of possible objective key features for in utero diagnosis of JSRD, we retrospectively compared posterior fossa measurements and ratios in prenatal MR imaging of the JSRD-affected and JSRD-nonaffected fetuses with those of a normal control group. Fetuses diagnosed by MR imaging as being JSRD-nonaffected by pre-

natal MR imaging were close to the control group in all of the obtained measurements. However, there was variation in measurements between the JSRD-affected group and normal fetuses at the pontomensencephalic junction. Unlike normal fetuses, the abnormally deep IP fossa in JSRD-affected fetuses was almost equal in its AP dimension to that of the dysgenetic isthmus (Figs 2*A* and 3*A*). Additionally, the average ratio of AP-to-transverse dimensions of the deformed fourth ventricle at the level of the dysgenetic isthmus in JSRD-affected fetuses was almost doubled (Fig 3*B*) in comparison to JSRD-nonaffected fetuses and control subjects. Ratios of measurements at the pontomesencephalic junction could be a potential objective key to enhance in utero diagnosis of JSRD, especially in cases with subtle MTS (Fig 2*A*).

A limitation of this study is that the imaging findings were determined by a single neuroradiologist, and thus the interrater reliability is unknown. Another limitation is the relatively small sample size that may influence the statistical reliability of the study, and other variables may be significant with a larger sample. The statistical power of this study ranges between 65% and 80%; by convention, 80% is the acceptable level of power. However, this study opens the door for further prospective and retrospective works to evaluate the diagnostic ability and accuracy of MR imaging findings and measurements in fetuses at risk of JSRD.

Counseling and management decisions for parents of a fetus diagnosed with fetal anomalies are multifactorial. The decision to terminate or to continue the pregnancy depends on the GA at diagnosis, the severity and type of the abnormality, presence of multiple anomalies, as well as social and religious views.[14] Fetal MR imaging increased the confidence in continuation of pregnancies with normal MR findings, and in this study all of them showed normal postnatal outcome. Abnormal fetal MR imaging findings enabled preparations for the birth of JSRD-affected children with respiratory abnormalities in a tertiary care hospital with a specialized neonatal care unit.

Conclusions

Fetal MR imaging can diagnose JSRD in at-risk pregnancies by detecting characteristic posterior fossa signs such as MTS. Measurements at the pontomesencephalic junction may enhance the accuracy of fetal MR imaging diagnosis of JSRD, especially in cases with subtle or equivocal findings.

References

1. Joubert M, Eisenring JJ, Andermann F. **Familial dysgenesis of the vermis: a syndrome of hyperventilation, abnormal eye movements and retardation.** *Neurology* 1968;18:302–03
2. Maria BL, Boltshauser E, Palmer SC, et al. **Clinical features and revised diagnostic criteria in Joubert syndrome.** *J Child Neurol* 1999;14:583–50
3. Chance PF, Cavalier L, Satran D, et al. **Clinical nosologic and genetic aspects of Joubert and related syndromes.** *J Child Neurol* 1999;14:660–66
4. Valente EM, Marsh SE, Castori M, et al. **Distinguishing the four genetic causes of Joubert syndrome-related disorders.** *Ann Neurol* 2005;57:513–19
5. Maria BL, Quisling RG, Rosainz LC, et al. **Molar tooth sign in Joubert syndrome: clinical, radiological, and pathological significance.** *J Child Neurol* 1999;14:368–76
6. Quisling RG, Barkovich AJ, Maria BL. **Magnetic resonance imaging features and classification of central nervous system malformations in Joubert syndrome.** *J Child Neurol* 1999;14:628–35
7. Gleeson JG, Keeler LC, Parisi MA, et al. **Molar tooth sign of the midbrain-hindbrain junction: occurrence in multiple distinct syndromes.** *Am J Med Genet* 2004;125A:125–34; discussion 117
8. Adamsbaum C, Moutard ML, Andre C, et al. **MRI of the fetal posterior fossa.** *Pediatr Radiol* 2005;35:124–40
9. Alorainy IA, Sabir S, Siedahmed MZ, et al. **Brain stem and cerebellar findings in Joubert syndrome.** *J Comput Assist Tomogr* 2006;30:116–21
10. Steinlin M, Schmid M, Landau K, et al. **Follow-up in children with Joubert's syndrome.** *Neuropediatrics* 1997;28:204–11
11. Hodgkins PR, Harris CM, Shawkat FS, et al. **Joubert syndrome: long term follow-up.** *Dev Med Child Neurol* 2004;46:694–99
12. Hafez M, El-Tahan H, Awadalla M, et al. **Consanguineous matings in the Egyptian population.** *J Med Genet* 1983;20:58–60
13. Zaki MS, Abdel-Aleem A, Abdel-Salam G, et al. **The molar tooth sign: a new Joubert syndrome and related cerebellar disorders classification system tested in Egyptian families.** *Neurology* 2008;70:556–65
14. Harper PS. **Genetic counseling and prenatal diagnosis.** *Br Med Bull* 1983;39:302–09
15. Baala L, Audollent S, Martinovic J, et al. **Pleiotropic effects of CEP290 (NPHP6) mutations extend to Meckel syndrome.** *Am J Hum Genet* 2007;81:170–79
16. Campbell S, Tsannatos C, Pearce JM. **The prenatal diagnosis of Joubert's syndrome of familial agenesis of the cerebellar vermis.** *Prenat Diagn* 1984;4:391–95
17. Anderson JS, Gorey MT, Pasternak JF, et al. **Joubert's syndrome and prenatal hydrocephalus.** *Pediatr Neurol* 1999;20:403–05
18. Ni Scanaill S, Crowley P, Hogan M, et al. **Abnormal prenatal sonographic findings in the posterior cranial fossa: a case of Joubert's syndrome.** *Ultrasound Obstet Gynecol* 1999;13:71–74
19. Aslan H, Ulker V, Gulcan EM, et al. **Prenatal diagnosis of Joubert syndrome: a case report.** *Prenat Diagn* 2002;22:13–16
20. Nyberg D, Jeanty P, Glass I. **Syndromes and multiple anomaly conditions.** In: Nyberg D, McGahan J, Pretorius D, et al, eds. *Diagnostic Imaging of Fetal Anomalies.* Philadelphia: Lippincott Williams & Wilkins; 2003:133–220
21. Hubbard AM, Simon EM. **Fetal imaging.** *Magn Reson Imaging Clin N Am* 2002;10:389–408
22. Poutamo J, Vanninen R, Partanen K, et al. **Magnetic resonance imaging supplements ultrasonographic imaging of the posterior fossa, pharynx and neck in malformed fetuses.** *Ultrasound Obstet Gynecol* 1999;13:327–34
23. Guibaud L. **Practical approach to prenatal posterior fossa abnormalities using MRI.** *Pediatr Radiol* 2004;34:700–11
24. Doherty D, Glass IA, Siebert JR, et al. **Prenatal diagnosis in pregnancies at risk for Joubert syndrome by ultrasound and MRI.** *Prenat Diagn* 2005;25:442–47
25. Fluss J, Blaser S, Chitayat D, et al. **MTS in fetal brain magnetic resonance imaging leading to the prenatal diagnosis of Joubert syndrome and related disorders.** *J Child Neurol* 2006;21:320–24
26. Grossman R, Hoffman C, Mardor Y, et al. **Quantitative MRI measurements of human fetal brain development in utero.** *Neuroimage* 2006;33:463–70
27. Chang CH, Chang FM, Yu CH, et al. **Three-dimensional ultrasound in the assessment of fetal cerebellar transverse and antero-posterior diameters.** *Ultrasound Med Biol* 2000;26:175–82
28. Garel C, Chantrel E, Elmaleh M, et al. **Fetal MRI: normal gestational landmarks for cerebral biometry, gyration and myelination.** *Childs Nerv Syst* 2003;19:422–25
29. Ivarsson SA, Bjerre I, Brun A, et al. **Joubert syndrome associated with Leber amaurosis and multicystic kidneys.** *Am J Med Genet* 1993;45:542–47
30. Van Drop DB, Palan A, Kwee ML, et al. **Joubert syndrome: clinical and pathological description of an affected male and a female fetus from the sibship.** *Am J Med Genet* 1991;40:100–04
31. Van Zalen-Sprock RM, van Vugt JM, van Geijn HP. **First-trimester sonographic detection of neurodevelopmental abnormalities in some single-gene disorders.** *Prenat Diagn* 1996;16:199–202
32. Wang P, Chang FM, Chang CH, et al. **Prenatal diagnosis of Joubert syndrome complicated with encephalocele using two-dimensional and three-dimensional ultrasound.** *Ultrasound Obstet Gynecol* 1999;14:360–62
33. Reynders CS, Pauker SP, Benacerraf BR. **First trimester isolated fetal nuchal lucency: significance and outcome.** *J Ultrasound Med* 1997;16:101–05
34. Souka AP, Snijders RJM, Novakov A, et al. **Defects and syndromes in chromosomally normal fetuses with increased nuchal translucency thickness at 10–14 weeks of gestation.** *Ultrasound Obstet Gynecol* 1998;11:391–400
35. Aslan H, Gungorduk K, Yildirim G, et al. **Prenatal ultrasonographic features of Joubert syndrome.** *J Clin Ultrasound* 2008;36:576–80
36. Carroll SGM, Porter H, Abdel-Fattah S, et al. **Correlation of prenatal ultrasound diagnosis and pathologic findings in fetal brain abnormalities.** *Ultrasound Obstet Gynecol* 2000;16:149–53
37. Pilu G, Segata M, Ghi T, et al. **Diagnosis of midline anomalies of the fetal brain with the three-dimensional median view.** *Ultrasound Obstet Gynecol* 2006;27:522–29
38. Pilu G, Visentin A, Valeri B. **The Dandy-Walker complex and fetal sonography.** *Ultrasound Obstet Gynecol* 2000;16:115–17
39. Limperopoulos C, Robertson RL Jr., Khwaja OS, et al. **How accurately does current fetal imaging identify posterior fossa anomalies?** *Am J Roentgenol* 2008;190:1637–43
40. Harper T, Fordham LA, Wolfe HM. **The fetal Dandy Walker complex: associated anomalies, perinatal outcome and postnatal imaging.** *Fetal Diagn Ther* 2007;22:277–81
41. Tilea B, Delezoide AL, Khung-Savatosvski S, et al. **Comparison between magnetic resonance imaging and fetopathology in the evaluation of fetal posterior fossa non-cystic abnormalities.** *Ultrasound Obstet Gynecol* 2007;29:651–59